

Failure mechanisms of Ni-H₂ and Li-Ion batteries under hypervelocity impacts

Miller, J. E.^a, Lyons, F.^b, Christiansen, E. L.^c and Lear, D. M.^{c1}

^aUniversity of Texas at El Paso, 500 W. University Ave., El Pas, TX 79968

^bHX5, NASA Johnson Space Center JETS contract, 2224 Bay Area Blvd, Houston, TX 77058

^cNASA Johnson Space Center, 1101 NASA Rd. 1., Houston, TX 77058

Abstract

Lithium-Ion (Li-Ion) batteries have yielded significant performance advantages for many industries, including the aerospace industry, and have been selected to replace nickel hydrogen (Ni-H₂) batteries for the International Space Station (ISS) to meet the energy storage demands. As the ISS uses its vast solar arrays to generate its power, the solar arrays meet their sunlit power demands and supply excess power to battery packs for power delivery on the sun obscured phase of the approximate 90 minute low Earth orbit. These large battery packs are located on the exterior of the ISS, and as such, the battery packs are exposed to external environment threats like naturally occurring micrometeoroids and artificial orbital debris (MMOD). While the risks from these solid particle environments has been known and addressed to an acceptable risk of failure through shield design, it is not possible to completely eliminate the risk of loss of these assets on orbit due to MMOD motivating a study into the failure consequences to the ISS. This paper documents the different failure modes for these two types of batteries under hypervelocity impact and the implications for spacecraft survivability when shielding is breached.

© 2017 The Authors. Published by Elsevier Ltd.

Peer-review under responsibility of the scientific committee of the 14th Hypervelocity Impact Symposium 2017.

Keywords: Lithium-Ion; Nickel hydrogen; Survivability; Hypervelocity

1. Introduction

Thermal runaway events have been experienced in terrestrial applications of the Li-Ion battery, and have been known to cause a fire that has the potential to spread to neighboring cells [1-3]. However, many aspects of the impact threat at ISS differ significantly from terrestrial failure scenarios requiring additional studies relevant to the ISS environment. Among the major differences is the configuration that is required for operation in space, the absence of an atmosphere and the impact speeds are far higher at the ISS. Owing to these differences, Li-Ion battery cells, that are representative of those selected for operation on the ISS, have been studied under conditions approximating orbital impacts.

As a basis of comparison of risk and as a result of the continued deployment, the predecessor nickel-hydrogen (Ni-H₂) cells have also been considered under similar conditions. For both types of cells, the representative shielding surrounding the battery pack is overwhelmed under the experimental impact conditions. This study has been directed by the NASA Johnson Space Center's Hypervelocity Impact Technology (HVIT) group for the International Space Station program office and the Boeing Company and performed at the 12.7 mm and 25.4 mm, two-stage, light-gas guns at the Remote Hypervelocity Test Laboratory in NASA Johnson Space Center's White Sands Test Facility, Las Cruces, NM.

2. Ni-H₂ Impact Experiments

An 81 A-hr, Ni-H₂ impact study has been performed on a legacy configuration of the ISS orbital replacement unit (ORU) battery assembly as shown in Fig. 1a. The experimental configuration of the ORU battery assembly in the test chamber is shown in Fig. 1b. This configuration is typical of the deployed ISS configuration and consists of thirty-eight cylindrical battery cells contained in a protective enclosure. The Ni-H₂ battery cells are constructed from Inconel

* Corresponding author. Tel.: +01-281-244-8093.

E-mail address: joshua.e.miller@nasa.gov

718 with minimum thicknesses in the cylinder of 0.8 mm and the dome of 0.65 mm. These Ni-H₂ batteries will continue to be deployed on the outside of the ISS even after they have been functionally replaced by the Li-Ion batteries; therefore, they represent a continued safety consideration for the ISS.

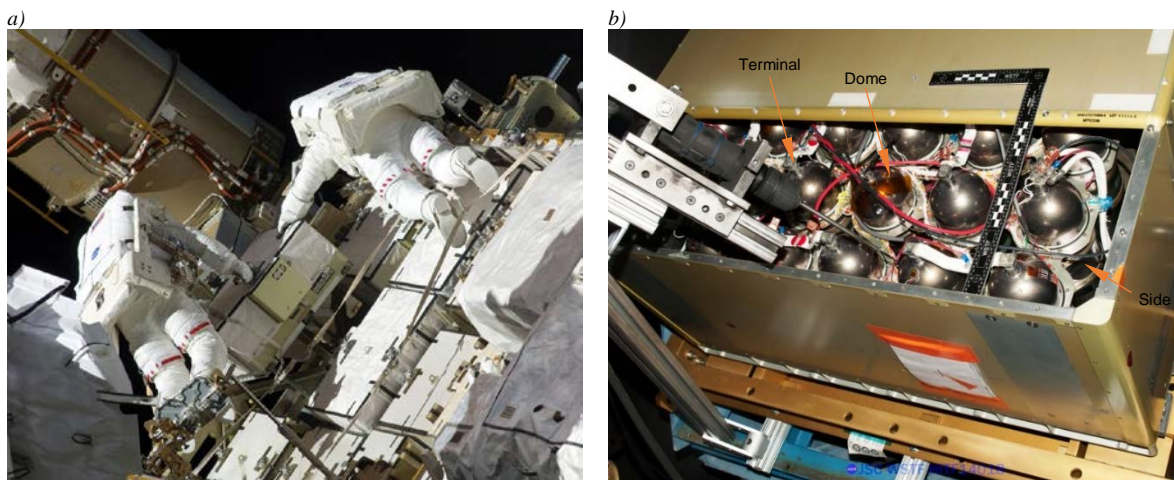


Fig. 1. (a) ISS Ni-H₂ battery ORU and (b) ORU subassembly with enclosure open.

The Ni-H₂ cell generates hydrogen gas in the free cell volume resulting from the chemical reactions that occur during charging, and in this design, the hydrogen accumulates up to a design pressure of 6 MPa, which indicates 100% state of charge (SOC) for the rated 81 ampere-hour (Ah). At this operational pressure, the designed burst factor for this cell is about six, and the cell casing is designed to leak before burst. In addition to the hydrogen gas, the cells also contain an aqueous potassium hydroxide (KOH) electrolyte solution. Because of this construction, two ISS safety concerns arise upon the failure of a cell due to impact: ejected fluids could react with materials around the cell and the impulsive nature of an impact could induce a fragmentation event rather than a leak. To address these concerns, an impact study has been performed to determine the failure mechanism for the Ni-H₂ cell after penetration and to assess if there are any adverse reactions with the electrolyte materials, thermal events or cascade failure responses.

To create a realistic impact scenario and containment environment, the studied Ni-H₂ cells are arranged and connected just as they are in operation and contained in a representative enclosure as seen in Fig. 1b. The cells are arranged on a square grid within the enclosure with an intercell separation of 25.4 mm. The cells are electrically connected to each other by aluminum bus bars attached between the cell terminals alternating between the top and bottom domes. The enclosure surrounding the cells consists of an aluminum honeycomb panel with 0.4 mm facesheets separated by a 12.7 mm thick honeycomb that is covered by a multi-layer insulation blanket (0.086 g/cm²). The minimum separation between the enclosure and a cell is nominally 33 mm. The top of the enclosure is 38 mm from the top of the dome, and the bottom of the enclosure is a large structural plate that is not consider a credible threat direction.

The Ni-H₂ impact conditions are summarized in Table 1. These experiments impacted through the enclosure, and have been targeted to consider three basic locations on the Ni-H₂ battery: in the dome, into the terminals on the top of the domes, and into the side. Various aluminum, Al2017-T4, and steel, SS440C, projectile diameters have been used in this study, at impact speeds of 7 km/s and impact angles of 0° and 45° to the normal of the honeycomb panel. None of the experiments resulted in fragmentation of the cells. No thermal events or cascading failures resulted in the loss of neighboring cells. The largest perforations are shown in Fig. 2a (HITF13144) and Fig. 2b (HITF13165). Generally, the response to cell perforation is that the Ni-H₂ cell vents and the voltage across the terminals declines until the cell could no longer maintain current over a load. In one case, the battery box cover deformed because the venting of the cell occurred so quickly that the pressure in the enclosure permanently deformed the cover.

Table 1. Ni-H₂ impact conditions with Al2017-T4 except where indicated.

Experiment #	Impact Location	Projectile Diameter (mm)	Impact Obliquity (°)	Impact Speed (km/s)	Cell Damage Summary (mm)
HITF13144	Dome	5.0	0	6.66	11.5 x 10.0 Perforation
HITF13145	Dome	4.0	0	6.86	1.0 x 1.5 Perforation
HITF13146	Dome	3.8	0	7.09	1.5 x 2.4 Perforation
HITF13147	Dome	3.4	0	7.09	2.4 x 3.5 Perforation
HITF13148	Dome	3.0	0	7.00	2.5 x 1.5 Perforation
HITF13149	Dome	2.8	0	7.19	No Perforation
HITF13151	Terminal	2.9	0	7.19	No Perforation
HITF13152	Terminal	3.1	0	7.12	No Perforation
HITF13153	Terminal	3.3	0	6.85	No Perforation
HITF13154	Terminal	4.2	45	7.13	1.6 x 1.2 Perforation
HITF13155	Terminal	3.0*	45	7.00	1.5 x 1.5 Perforation
HITF13158	Dome	5.0	45	7.13	2.0 x 2.0 Perforation
HITF13159	Dome	4.0	45	7.00	No Perforation
HITF13160	Dome	4.2	45	7.07	1.8 x 08 Perforation
HITF13162	Terminal	5.0	0	7.05	7.5 x 7.0 Perforation
HITF13163	Terminal	4.8	0	7.07	No Perforation
HITF13164	Terminal	5.1	0	7.04	3.0 x 1.0 Perforation
HITF13165	Terminal	3.8*	0	6.87	18.0 x 8.0 Perforation
HITF13174	Side	4.1	45	7.04	1.0 x 4.0 Perforation
HITF13175	Side	3.9	45	7.04	No Perforation

*SS440C steel projectiles

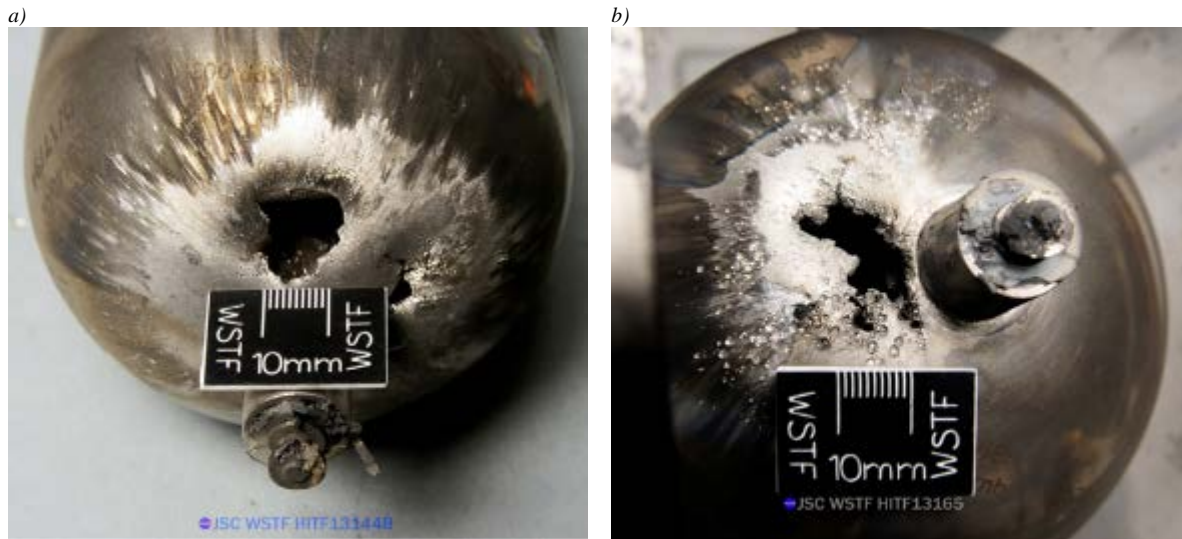


Fig. 2. Most significant observed damage of the Ni-H₂ cells (a) HITF13144 and (b) HITF13165.

3. Li-Ion Impact Experiments

An impact study of a 134 A-hr, Li-Ion cell, shown in Figure 3a, has been performed in a representative configuration of the ISS ORU as seen in Figure 3b. Similarly, an impact study has also been performed with the 72 A-hr, Li-Ion cell, shown in Figure 3c, in its ISS representative configuration of the ISS ORU as seen in Figure 3d. Like the Ni-H₂ cells, the Li-Ion cells are also contained in an aluminum honeycomb panel ORU box. The aluminum honeycomb panel is separated from the top of the Li-Ion cells by 91 mm for the 134 A-hr and 155 mm for the 134 A-hr. The Li-Ion configuration also includes additional protective materials internal to the enclosure, which includes 19 mm Solimide foam spacer followed by two sheets of Nextel 312 AF62 fabric. These protective materials are repeated with a total of 38 mm spacing foam and two sets of two Nextel sheets. These added shield materials increase the protection of the Li-Ion cells; thus, significantly decreasing the likelihood of failure of the cells from an impact.

a)

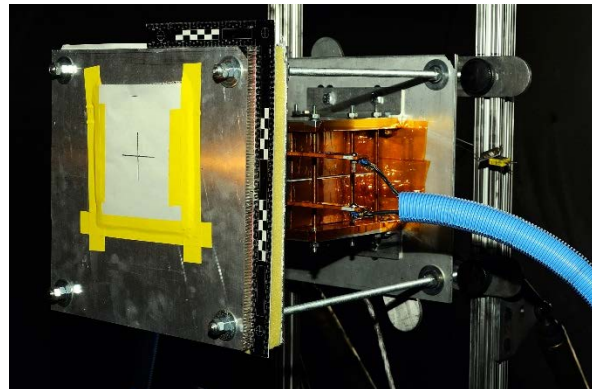
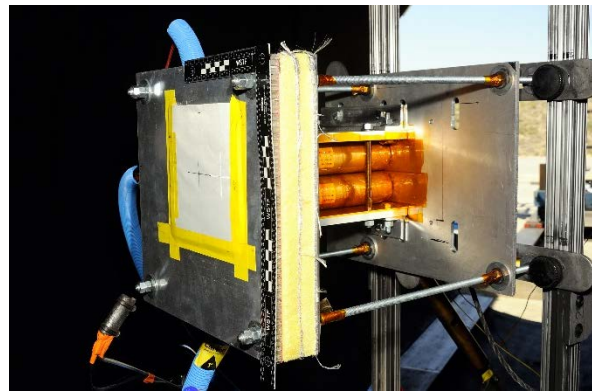


Table 2. Li-Ion cell impact conditions.

Experiment / Cell Type	Impact Location	Projectile Diameter (mm)	Impact Obliquity (°)	Impact Speed (km/s)	Cell Damage Summary
HITF12143 134 A-hr	Terminal	10.0	0	6.86	Primary cell-Perforated, peak of 184°C Secondary cell-No ignition or thermal runaway
HITF12144 72 A-hr	Terminal	10.0	0	7.02	Primary cell-Perforated, peak of 194°C Secondary cell- Thermal runaway peaking at 531°C
HITF12145 134 A-hr	Side	10.0	30	7.05	Primary cell-No Perforation Secondary cell-No Perforation
HITF12146 72 A-hr	Side	10.0	30	7.02	Primary cell-No Perforation Secondary cell-No Perforation
HITF12147 134 A-hr	Side	13.5	45	6.88	Primary cell-Perforated, peak of 193°C Secondary cell- Thermal runaway peaking at 315°C
HITF12148 134 A-hr	Terminal	10.0	0	7.19	Primary cell-Perforated, no ignition Secondary cell-No thermal runaway

The impact locations are typically at the terminal end of the battery cells, although, some shots to the side of the Li-Ion battery have also been performed. Both cell configurations demonstrated similar failure results. When penetrated, the impacted Li-Ion battery typically increases in temperature while the cell contents are ejected. The neighboring cell will in most cases increase in temperature, but only occasionally will the temperature increase substantially and result in failure of the undamaged cell. An example of such a cascade is shown in Fig. 4 of a sequence of images of the Li-Ion battery response from HITF12143. The first three frames are on one second intervals, and the remaining five frames are on two second intervals. As can be seen, this experiment resulted in a visible deflagration as the impacted cell contents are energetically ejected over several seconds following cell penetration.

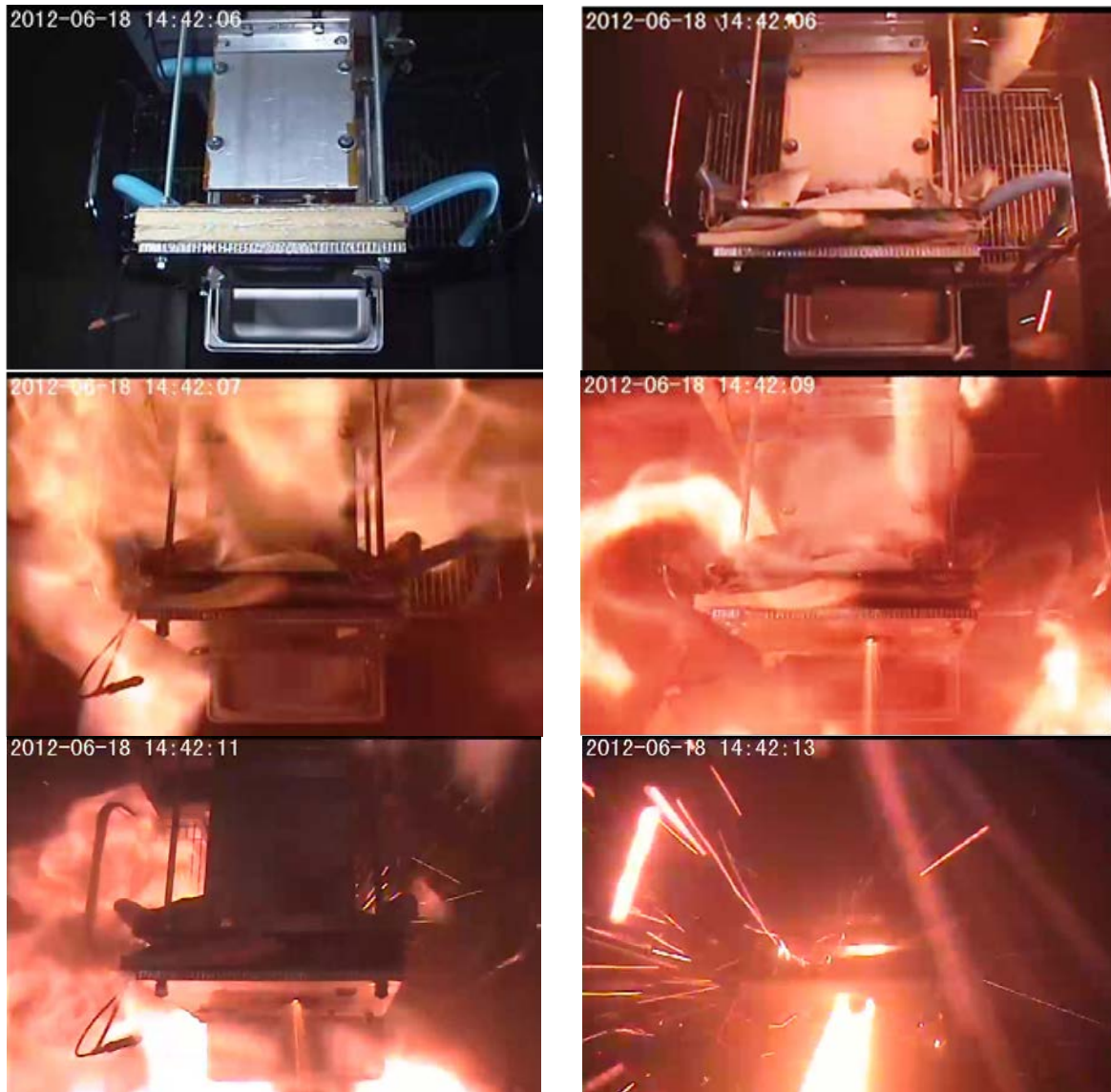


Fig. 4. HITF12143 visible video frames at 1s and then 2s intervals after impact.

The aluminium honeycomb panel in front of the cell, Figure 5a, was severely melted due to the expelled cell material; however, the neighbouring cell did not transition into thermal runaway in this impact experiment. Whenever a cells contents eject, significant quantities of metallic flakes are formed following cooling of the molten material as seen in Figure 5b with similar metallic flakes spread throughout the target chamber. These flakes would contribute to the orbital debris environment in an operational environment release.

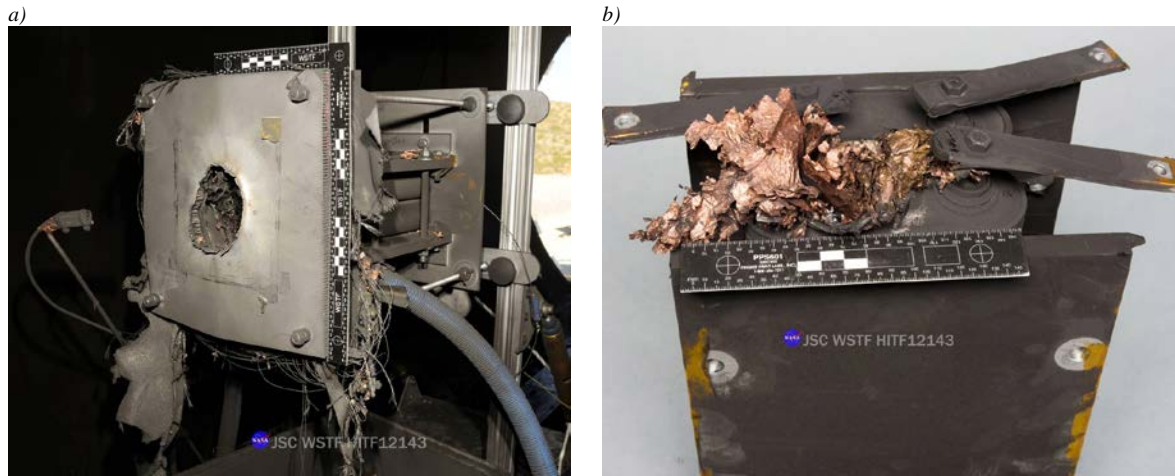


Fig. 5. HITF12143 damage photography of a) representative enclosure and b) ejected cell material that remained with the cell.

4. Conclusions

The use of rechargeable batteries in orbital spaceflight requires consideration of the uncontrolled energy release from a cell, which is dependent on the type of cell. Impact experiments have evaluated the failure mechanisms of the fully charged Ni-H₂ battery cell and Li-Ion battery cell. For the operational design of the Ni-H₂ battery like those used on the ISS, the hydrogen gas will vent on perforation of the battery vessel; but unusual thermal events or catastrophic rupture did not occur. The ISS Ni-H₂ battery cells have a relatively high burst factor of 6. When pressurized battery cells are used in other spacecraft, attention to the burst factor of the cell should be taken into account.

Impact experiments on Li-Ion battery cells demonstrated an energetic release when shielding is overmatched and the cell is penetrated. The impacted cell will typically overheat and will vent/eject the internal contents of the cell, including molten metal, rapidly after impact (within a few seconds). In some cases, the venting material will auto-ignite, even in the vacuum environment of the test chamber. Depending on the design of the battery cell enclosure, neighboring Li-Ion cells can also experience increases in temperature and can fail due to thermal runaway.

Shielding for batteries should be selected based upon the type of cell to be protected, typical failure modes and the acceptability for loss of battery cells. Supplemental shielding for Li-Ion batteries should be designed to meet survivability requirements without allowing perforation of the cell wall. Shield and battery designs should be verified by test to ensure they meet protection requirements.

Acknowledgements

The authors wish to gratefully acknowledge the International Space Station program office and its prime contractor, the Boeing Company, for making available the research specimens and funding the research, and the NASA White Sands Test Facility's Remote Hypervelocity Impact Laboratory for the seamless execution of this research. University of Texas at El Paso support sponsored under Jacobs JETS contract EN41520TMS.

References

- [1] C. Mikolajczak, M. Kahn, K. White, R. T. Long, Lithium-ion batteries hazard and use assessment, Fire Protection Research Foundation Report (2011).
- [2] N. Williard, W. He, C. Hendricks, M. Pecht, Lessons learned from the 787 Dreamliner issue on lithium-ion battery reliability, *Energies*, 6 (2013) 4682-4695.
- [3] G. Kim, K. Smith, J. Ireland, A. Pesaran, Fail-safe design for large capacity lithium-ion battery systems, *J. Pow. Sys.* 210 (2012) 243-253.
- [4] J-M. Tarascon and M. Armand, Issues and challenges facing rechargeable lithium batteries, *Nature*, 414.6861 (2001): 359-36